Study AB-Initio of New Unconventional Topological in Half and Full Heuslers Materials

Chahrazed M[1,2], Ali M[*1,2], Yamina M[1,2], Moued M[3], Youcef C[2], Mestfa D[1,2] and Ali Z[1]

[1]Computational Physics of Materials Laboratory, Djillali Liabes University of Sidi Bel-Abbes, Sidi Bel-Abbes, Algeria
[2]University Centre Ahmed Zabana of Relizane, Algeria
[3]University Center of El-bayed, Algeria

[*]**Corresponding Author:** Ali M, Computational Physics of Materials Laboratory, Djillali Liabes University of Sidi Bel-Abbes, Sidi Bel-Abbes and University Centre Ahmed Zabana of Relizane, Algeria, Tel: +2130673006726, E-mail: mirali1205970@gmail.com

ABSTRACT

Predicting topological numbers may be the key to understand these materials which have exhibited fascinating properties. We have carried out this comparative study between two materials of Heusler nature to clarify this side. To meet this requirement, we examine the topological indices of the surface of the two Heuslers materials. Therefore we follow a method based on Density function theory (DFT) combined with another weak link-based method for determining topological indices. This method is very efficient and widely used in ab-initio studies to subtract Chern number "C", topological number "Z2" and Abnormal Hall Effect (AHE).

Keywords: C: Chern Number; Z2: Topological Number; AHE: Spin Orbital Coupling

Introduction

The discovery of topological insulators opens a new window of the future of the advanced electronic industry such as spintronic components and quantum computers [1,2]. The notion of a topological insulator is simple, the material has an electronic insulating structure in bulk butconductive on the surface. In other words, in the physical language it is a material that has metallic surface states protected by time inversion symmetry 'TRS', the latter condition lets the material retain its properties under significant disturbances without breaking its symmetry [1,2]. Studies have classified non-magnetic type Z2 insulators into two categories, one topological Z2 -dd (topological) and the other ordinary Z2 -even (ordinary).In 2D materials, Z2 - "odd class" is known by its peers of Kramer's helical edge states, on the other hand, the 3D system is characterized by theodd number of Fermi loops of the surface band which contains certain points of high symmetry in Brillouin Zone (BZ) [3]. All these studies stay frozen until the realization of a quantum system witha spin hall effect in HgTe in 2007 [4] other studies and realizations follow this approach [5-8]. The fascinating properties of these types of topological materials lead research into metals, Half- Heusler, and also into insulators [9-11]. A semi-Dirac semi-metal is characterized by the crossing point of a linear band and a quadratic band in the space of the pulses forming a 1-D circle on the surface. But for Weyl semi-metal, Fermi's surface forms an arc as a surface, instead of a closed circle [9,10]. These studies answer a major question about arcs formation and also show that it has different forms of arcs. A recent study shows that large arcs that appear on surfaces can act as catalysts [12].

Method

We have used the Tight-Binding (TB) method combined with the Wannier wave function implantedon Wannier90 code [13] to verify some topological properties of our materials. The initial computation was carried out by the Wien2k code [14] and espresso Quantum [15]. We used the Lowdensity Approximation (LDA) [16] to describe the correlation exchange effects [17]. In the "TB" method, we consider the atomic interactions are quite weak in this crystal. In this way, the Hamiltonian only couples the orbital of the atomic sites close to each other, so that other couplings can be neglected. So, all these applications are done in a Hilbert space that acts on a network systemthat will distort one or two Hamiltonians with the existence of a "gap" at the Fermi level. It is logical not to close a course of time so we can say that we have an important symmetry during time reversal. In other words, if we change the two Hamiltonians connected adiabatically to each other without closing the bands in this case we say that the topological properties of the Hamiltonian are protected. This topological notion is characterized by a topological invariant which takes values in Z2, which we will call the index Z2. For several bands, we need Wilson loop method [18] based on the angle "θ". Once the angle "θ" has been calculated all topological numbers will be determined. The topological properties have been calculated within the context of the "Green" function method [19] which is implemented in Wannier-Tools [20]. An important note all the physical parameters have been calculated and compared in Table [1-2].

	Wyckoff positions	a(A°)	β(GP)	β'
NbRhSb-HH (SG 216 F- 43m)	X=4a (0, 0, 0) Y=4c (1⁄4, 1⁄4, 1⁄4) Z=4b (1⁄2, 1⁄2 ,1⁄2)	6.10 this work 6.17 Exp [28]	4.64 this work	186 this work
Ni2SnZr-FH (SG-225 Fm- 3m)	Y=4a (0, 0, 0) X=4c (1⁄4, 1⁄4, 1⁄4) Z=4b (1⁄2, 1⁄2 ,1⁄2)	6.17 this work 6.24 LDA [27] 6.27 Exp[27]	4.38 this work	120 this work 149 [27]

Table 1: Structural parameters calculated, compared with other researches of the NbRhSb andNi2SnZn compounds with his Wyckoff positions

Chern number for 6 planes	For NbRhSb	Z2 number for 6 planes	For NbRhSb
k1=0.0, k2-k3 plane:	1	k1=0.0, k2-k3 plane:	0
k1=0.5, k2-k3 plane:	-2	k1=0.5, k2-k3 plane:	1
k2=0.0, k1-k3 plane:	0	k2=0.0, k1-k3 plane:	1
k2=0.5, k1-k3 plane:	0	k2=0.5, k1-k3 plane:	1
k3=0.0, k1-k2 plane:	-2	k3=0.0, k1-k2 plane:	1
k3=0.5, k1-k2 plane:	1	k3=0.5, k1-k2 plane:	1

Table 2: Chern number and Z2 topological index for 6 plan of NbRhSb

Band structure analysis

The band structures of Ni2SnZr and NbRhSb were calculated with and without spin-orbit coupling (SOC), we obtained an aperture in the bands of few "mev" 60mev and 160mev in the semi-core bands of the two materials when we applied the "SOC" (Figure 1b and e). This is a strong indication of the existence of topological state [8-10]. This remark also appeared as a magenta spot on the surface state spectrum illustrated in Figure 1c and f. Regarding the explosion of the two bands of Ni2SnZr is mainly due to the atomic bond Ni-Ni. The red and blue band are dominated by the same state |d_eg+>, therefore, the two bands bear the same sign and the repulsion effect plays a big role ithe separation of the two bands. For NbRhSb the separation of the two bands is due to a set of states which carry the same charge signs |d_eg- + d_t2g+> of the two atoms Nb and Rh. This effect has been seen in other studies that occur along at point symmetries "Γ" and "M" due to the Rashba effect and the lack of inversion of symmetry, other explosions that appeared at the "K" point are also due to Zeeman -Type spin splitting [21].

Topological properties

The calculate of the Wannier Charge Centers "WCCs" or Wilson loops without SOC of NbRhSb illustrated in Figure 2g shows that the number of curves arbitrarily crosses all the reference lines and odd times which means that the phase is non-trivial and Z2 topological indices calculated take 6 values between 0 and 1 following each plan of 3D (see table2), while Z2 topological indices of Ni2SnZr equals zero for six plan of 3D is a correspondence of a trivial topological phase. Our analysis of "WCCs" consists on the "Soluyvanov-Vanderbilt" method [24] whom reciprocal lattice vectors w1, w2, w3 are represented as follows kw1 +tw2 and 0.5w3 +kw1 + tw2 for k, t ∈ [0,1], which cover the six parallelepiped faces in the space of moments and each vertex represents an invariant time of time inversion. Each face of this parallelepiped is interpreted as a two-dimensional periodic system if the Hamiltonian is considered as a function of two moments, in particular, each face can assign an index Z2 topological indices whose index is denoted with v=v1 +v2 mod2 follows Soluyvanov Vanderbilt method. For v to be non-trivial, one of the faces must be trivial while the opposite face is non-trivial in 3D. Here Wannier charge centre "WCCs" flow as a function of k during one cycle for NbRhSb and the crystal momentum in the direction of w2 plays the role of k. The "WCCs" separate and reconnect in a non-trivial way, switching partners after a cycle in the interval of "WCCs"∈ [0, 0.5] and at point k = 0.25. Figure 2-(g) of "WCCs" clearly shows the flux of the Wannier charge centre as a function during a cycle for NbRhSb in bulk and surface. Now it is easy to analyze the plans: taking the plan [k1-k3] with k1 = 0 and k1 = 0.5 and v it is the number of winding which has the same number equal to 1 so it is trivial in this plan (see Figure 1h), in the case of the plan [k2-k3] and v take two different values we get Z2 =1 so this face contains a non-trivial topological insulator where the curve is protected by Time-Reversible Symetry TRs, the same thing for the plan [k1-k2] is trivial. For 3D insulators, we have four different indices as illustrated on table2 V0 (vx,vy,vz) where V0 represents the total number of Z2 topological indices in the direction x, y, z. If the number of two same plans are different we have Z2=1 and if we have the same number therefore Z2=0.In 3D, if we only have one non-trivial plan among the six plans, then the material is non-trivial. If band inversion happens an even number of times or it happens around an even number of Time Reversal Invariant Momentum points, we obtain a trivial insulator phase and Z2 =0. If we have Z2 =0 after the summation on the band index n due to the degeneration of Kramers see Figure 3a in K direction, in this case, the occupied electronic states must be even, ψ1 and ψ2 these two wave functions are called the Kramers pairs [21]. We have calculated also the Chern number of Ni2SnZr which is equal to zero, whom the bands are degenerate by an even number and have a dispersion in all directions around, which means that the total topological charge of the valence bands is zero. The number of "Chern" of NbRhSb has been calculated and illustrated in Table 2. In 3D,
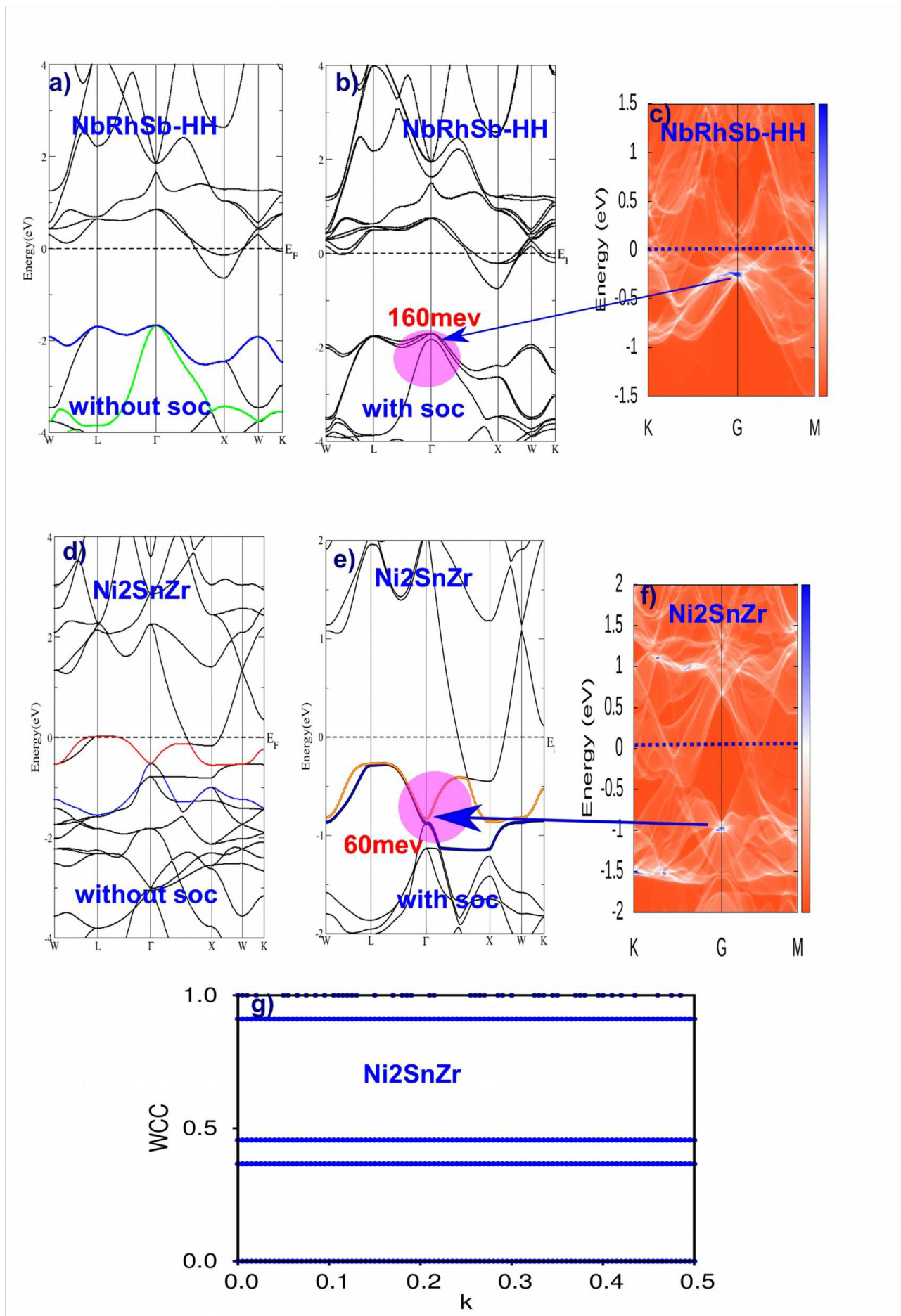
Figure 1: a-b-d-e) Ni2SnZr and NbRhSb with and without spin orbit coupling; **c-f)** Spectral function along kz direction on surface calculated withDFT method; **g)** Wannier charge centers evolution loops of Ni2SnZr
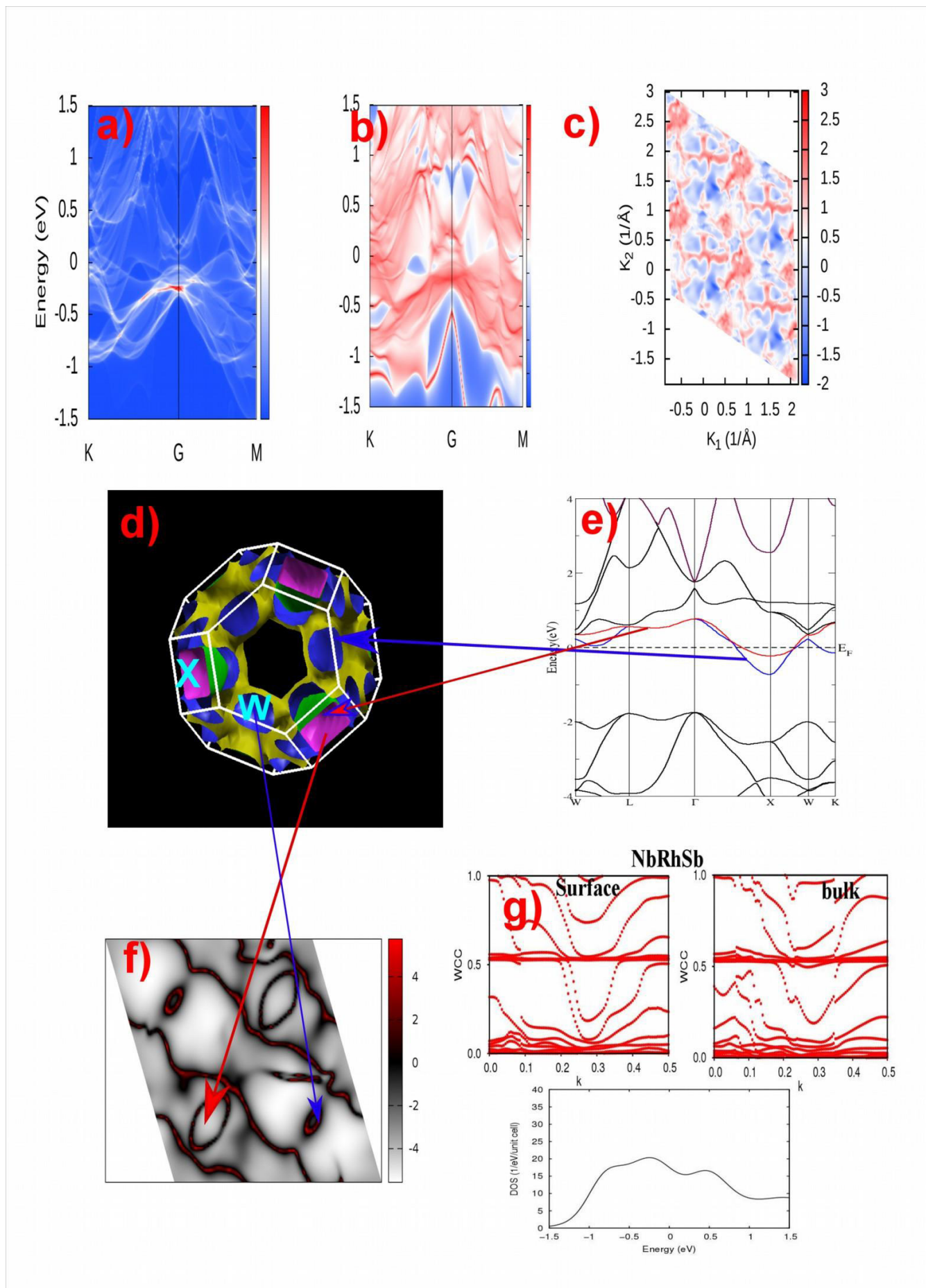
Figure 2: Intensity **(a)** and curvature intensity **(b)** plots of the ARPES data along with K–G–M. Forcomparison, we plot the calculated bands along with W–Γ–X – K; **(d,e,f)** represented 2D FS and 3Dwith yellow connected band; **(g)** represents Wannier charge centers Evolution "WCC" or Wilson loops in Bulk and surface with DOS of NbRhSb

the calculations show that each plan has its non-zero topological number, and Chern'sopposite numbers mean that there is an "anti-symmetric surface". It is clear that the Fermi surfaceof NbRhSb Figure 2e presents two adjacent bands (blue and red) which intersect the Fermi levels twiceat the same point of high symmetry "X", and the number of Chern takes two values C=+1 and C=- 2, this means that these twice pockets do not have the same chirality but one superimposed on the other [30] that is to say, the two blue and red bands cross in the point "X" with the topological charges C=+1 and C=-2 respectively in the helicity 0. The dispersion of the blue band projected along on the all high symmetry points cuts the Fermi level a lot of points, near "W" point the band forms a cone which takes the same value of number Chern C=+1 in two different plan [k1-k2] and [k2-k3] suggest a chiral fermion [30,31]. Therefore, the number of Chern must change from a positive phase to a negative phase during the variation of energy at the surface forming a robust non-trivial surface state [30] and this two cone are cnfined in this band. The non-connectivity of bands in the first Brillouin Zone in Ni2SnZr generates topologically trivial material with zero Chernnumber, zero topological number and weak topological Fermi arc surface [30]. The surface states ofNi2SnZr is trivial because they do not connect across the bulk band-gap (Figure 3b,c and d) [32]. Figure 4 (a) clearly shows the six nodes and the six Weyl points with arc energy equal to zero [33,34]. The increase of the energy with 0.06ev pushes its lobes of is distinguished and forms three points of the Weyl point this means that the superimpositions of the Weyl points are disappeared, another small increase in energy of   0.04ev makes these points a superimpose a second time and take place of the points of high symmetry of the first BZ these results are confirmed by Hongming Weng et al. (Figure 4b and c) [33-35].
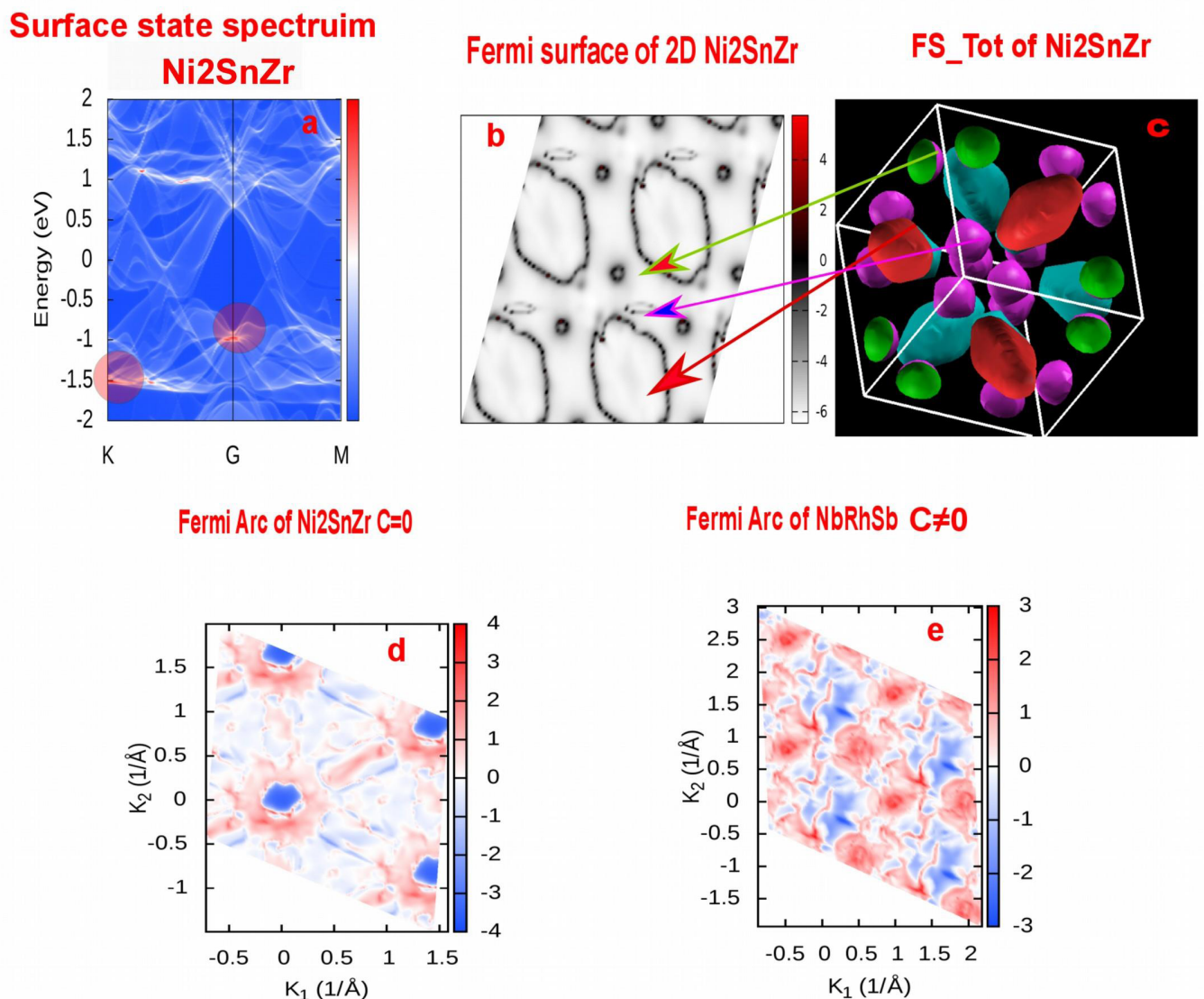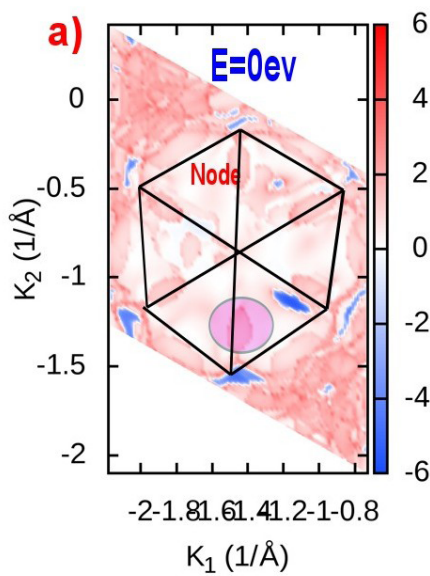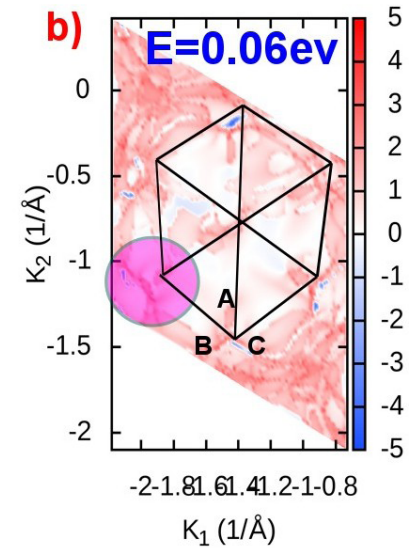

Figure 3: a) Represented surface state spectruim with opening "gap" at high symmetry points "G" and "K" represented by a red spot; **b)** and **c)** Fermi surface 2D and 3D of Ni2SnZr with absence of connected band near level Fermi; **d)** and **e)** represented arc Fermi on surface [110] with chernnuber C=0 for Ni2SnZr and C=0 for NbRhSb

The arc connecting to superposed Weyl points

The arcs form a trimer.
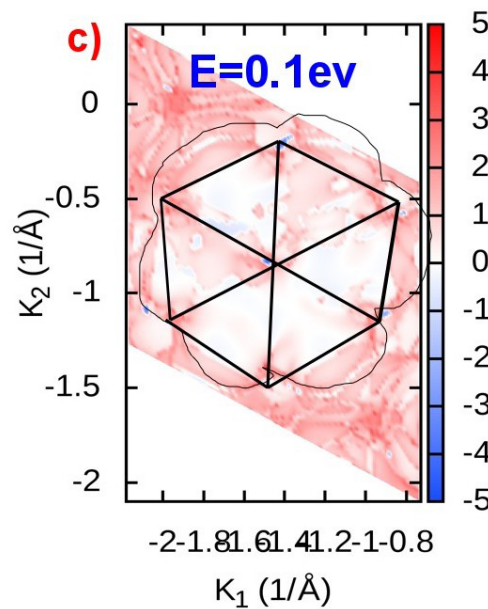
The arcs form a hexamer.

Figure 4: Surface states show Arc bulk the lobes of Nodal lines in the first BZ with different energiescalculated without SOC, whereas Weyl points "WPs" appear in the plane **a)** Arc connectingsuperposed Weyl points; **b)** Arc from a trimer; **c)** Arcs from hexamer and energy distribution curves near the Weyl point

Anomalous Hall Conductivity

The abnormal Hall Effect requires a combination of magnetic polarization and spin-orbit couplingto generate a finite Hall voltage these two properties are present in NbRhSb and Ni2SnZr. TheKubo Formula can be characterized by two terms, the first contribution is the intra-band transitions of the states close to the Fermi level or the non-diagonal elements of the Green's function, and the second contribution is the states located below the Fermi level or the deep states which are often called the topological contribution because the contribution of "σxy" depends explicitly on the nature of the quantum states | n, k> via the gauge potential [29]. In our study of intrinsic AHC, we use the Kubo relation according to the [110] plans (Figure 4), because this plan is the most relevant in experimental studies, and we focus on the intrinsic part of the Berry curvature.

$$\sigma_{xy} = \frac{e^2}{h} \sum_{n=1}^{occ} \int_{BZ} (d^3k/(2\pi)^3) f(\zeta(k) - \mu) \Omega_{n,b}(k) = n\frac{e^2}{h}$$

Kubo's Formula clearly shows that Hall's conductivity is directly related to Berry's curvature and also gives a strong indication of the underlying space [25]. If the number "n" is an integer, it means that the "σxy" conductivity is quantified and is related to the first Chern index. This number has a relation with the Landau levels filled and each level has a Chern index. According to the relationship, it is clear that this index plays an important role in completely filled strips. These saturated bands can conduct current even if it is filled [26]. On the other hand, each plan which is between two Weyl point contributes to the Chern number, in other words, the plans outside the Weylpoints are Chern numbers equal to Zero [26]. In this case, the AHC calculations must be between these Chern numbers provided that the volume of the Fermi surface exists and this area will be separated by two regions, one near Γ and the other far from Γ. The equation will be zero if only is field B parallel to the" XY" plan. Our Figures clearly illustrate the calculations of the Hall conductivity for the two materials as a function of energy or chemical potential when B revolves around the XY plane. Figure 5a clearly shows that the curve of NbRhSb is smooth because it fulfils all the conditions of the Kubo formula on the contrary for the curve of Ni2SnZr which presents a lot of peaks and losses its smoothing. Figure 5b shows the sharp increase in the height of the peak in the negative direction of around of value 1.25eV for Ni2SnZr this is a consequence of the large separation of the Weyl point along the y axis when the angle increases from zero and the large separation between pockets in the first BZ (Figure 3). This remark is very clear on the Fermi surface Figure 3c and b where the cones are far from each other and are not connected which is why the curve takes these sharp peaks, therefore the plans are outside the Weyl point, and the number of Chern equals zero. On the other hand, the curve of NbRhSb rises smoothly which means that the Weyl points are close to each other and that they are connected by a band see FS Figure 2d and f.
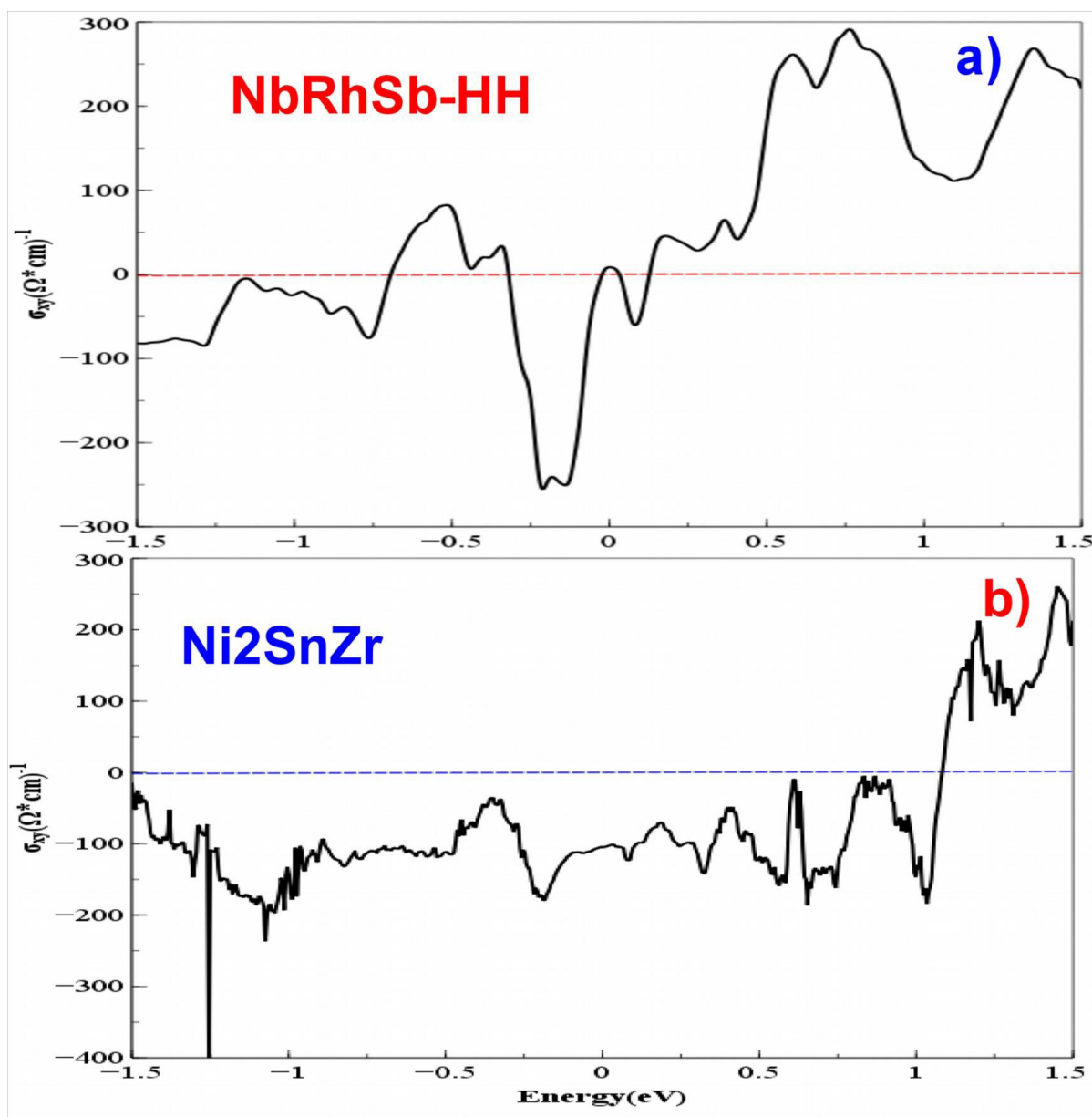

Figure 5: (a,b) calculation of Anomalous Hall Conductivity of NbRhSb and Ni2SnZr

Conclusion

We have successfully obtained the topological indices of NbRhSb and Ni2SnZr in the context of DFT combined with dynamic methods. Calculations of both topological indices and Chern numbersshow that NbRhSb is a non-trivial material while Ni2SnZr is trivial. NbRhSb exhibits a robust Fermi surface with Weyl points "WPs" which connects the valence band with conduction bands but Ni2SnZr has a weak arc Fermi surface with an absence of the connected band. The calculations of AHC was obtained with success through σxy as a function of energy for both materials.

References

1. Hasan MZ, Kane CL (2010) Colloquium: Topological insulators. Rev Mod Phys 82: 10.1103/RevModPhys.82.3045.

2. Qi XL, Zhang SC (2011) Topological insulators and superconductors. Rev Mod Phys 83: 10.1103/RevModPhys.83.1057.

3. Kane CL, Mele EJ (2005) Z2 Topological Order and the Quantum Spin Hall Effect. Phys Rev Lett 95: 10.1103/PhysRevLett.95.146802.

4. König M (2007) Quantum Spin Hall Insulator State in HgTe Quantum Wells. Science 318: 766-70.

5. Mondal C, Kumar S, Pathak B (2018) Topologically protected hybrid states in graphene–stanene– graphene heterojunctions. J Mater Chem C 6: 1920-5.

6. Xu Y (2013) Large-Gap Quantum Spin Hall Insulators in Tin Films. Phys Rev Lett 111: 10.1103/PhysRevLett.111.136804.

7. Hsieh D (2009) Observation of Time-Reversal-Protected Single-Dirac-Cone Topological- Insulator States in Bi 2 Te 3 and Sb 2 Te 3. Phys Rev Lett 103: 10.1103/PhysRevLett.103.146401.

8. Barman CK, Alam A (2018) Topological phase transition in the ternary half-Heusler alloy ZrIrBi. Phys Rev B 97: 10.1103/PhysRevB.97.075302.

9. Liu ZK (2014) Discovery of a Three-Dimensional Topological Dirac Semimetal, Na3Bi. Science 343: 864-7.

10. Xu (2015) Discovery of a Weyl fermion semimetal and topological Fermi arcs. Science 349: 613-7.

11. Bian G (2016) Topological nodal-line fermions in spin-orbit metal PbTaSe 2. Nat Commun 10.1038/ncomms10556.

12. Yang Q, Li G, Manna K, Fan F, Felser C, et al. (2020) Topological Engineering of Pt-Group-Metal-Based Chiral Crystals toward High-Efficiency Hydrogen Evolution Catalysts. Adv Mater 32: 10.1002/adma.201908518.

13. Wu QS, Zhang SN, Song HF, Troyer M, Soluyanov AA (2018) WannierTools: An open-source software package for novel topological materials. Comput Phys Commun 224: 405.

14. Blaha P, Schwarz K, Madsen G, Kvasnicka D, Luitz J (2001) WIEN2k, An Augmented Plane Wave + Local Orbitals Program for Calculating Crystal Properties.

15. Giannozzi P, Baroni S, Bonini N, Calandra M, Car R, et al. (2009) QUANTUM ESPRESSO: a modular and open-source software project for quantum simulations of materials. J Phys Condens Matter 21: 395502.

16. Kohn W, Sham LJ (1965) Self-Consistent Equations Including Exchange and Correlation Effects. Phys Rev 10.1103/PhysRev.140. A1133.

17. W Kohn, LJ Sham (1969) Self-Consistent Equations Including Exchange and Correlation Effects. Phys Rev 140: A1133.

18. Yu R, Qi XL, Bernevig A, Fang Z, Dai X (2011) Equivalent expression of Z 2 topological invariant for band insulators using the non-Abelian Berry connection. Phys Rev B 84: 75119.

19. Lopez Sancho MP, Lopez Sancho JM, Rubio J (1985) Highly convergent schemes for the calculation of bulk and surface Green functions. J Phys F: Met Phys 15: 851.

20. Wu Q, Zhang S, Song HF, Troyer M, Soluyanov AA (2017) WannierTools: An open-sourcesoftware package for novel topological materials. Computer Physics Communications 10.1016/j.cpc.2017.09.033.

21. Wen-Zhi X, Xiao G, Rong Q-Y, Wang L-L (2019) Oxygenation-Induced Two-Dimensional Topological Insulators in Antimony Arsenide. Phys Status Solidi 10.1002/pssr.201900146.

22. Fu L, Kane CL (2006) Time Reversal Polarization and a Z_2 Adiabatic Spin Pump. Phys Rev B 74: 195312.

23. Yu R, Qi XL, Bernevig A, Fang Z, Dai X (2011) An equivalent expression of Z2 Topological Invariant for band insulators using Non-Abelian Berry's connection. Phys Rev B 84: 10.1103/PhysRevB.84.075119.

24. Soluyanov AA, Vanderbilt D (2011) Computing topological invariants without inversion symmetry," Physical Review B - Condensed Matter and Materials Physics 83: 10.1103/PhysRevB.83.235401.

25. Choi Y (2020) Zeeman-splitting-induced Topological Nodal Structure and Anomalous Hall Conductivity in ZrTe5. Phys Rev B 10.1103/PhysRevB.101.035105.

26. Thouless DJ, Kohmoto M, Nightingale MP, den Nijs M (1982) Quantized hall conductance in a two-dimensional periodic potential. Phys Rev Lett 49: 405-8

27. Serdar O (2013) Band gap and stability in the ternary intermetallic compounds NiSnM (M =Ti, Zr, Hf): A first principles study. doi 10.1103/PhysRevB.51.10443.

28. Evers CBH, Richter CG, Hartjes K, Jeitschko W (1997) Ternary transition metal antimonides and bismuthides with MgAgAs-type and filled NiAs-type structure. Journal of Alloys and Compounds 252: 93-7.

29. Crépieux A, Bruno P (2001) Theory of the anomalous Hall effect from the Kubo formula and the Dirac equation. Phys Rev B 64: 10.1103/PhysRevB.

30. Tang P, Zhou Q, Zhang S-C (2017) Multiple Types of Topological Fermions in Transition Metal Silicides. Phy Rev Lett 119: 206402.

31. Rao z, Li H, Zhang T (2019) Observation of unconventional chiral fermions with long Fermi arcs in CoSi. Nature 567: 496-9.

32. Huang S-M, Xu S-Y (2013) A Weyl Fermion semimetal with surface Fermi arcs in the transition metal monopnictide TaAs class. Nat Communi 6: 10.1038/ncomms8373.

33. Lv BQ, Feng Z-L (2017) Observation of three-component fermions in the topological semimetal molybdenum phosphide. Nat 627: 10.1038/nature22390.

34. Weng H, Fang C (2016) Coexistence of Weyl fermion and massless triply degenerate nodal points. Phy Rev B 94: 165201.

35. Zhu Z, Winkler GW, Wu QS, Li J, Soluyanov AA (2016) Triple Point Topological Metals. Phys Rev X 6: 031003